Analytical Methods

Accepted Manuscript

This article can be cited before page numbers have been issued, to do this please use: H. Kholafazad kordasht, M. Hasanzadeh, M. Moosavy, J. Soleymani and A. Mokhtarzadeh, *Anal. Methods*, 2019, DOI: 10.1039/C9AY01185D.

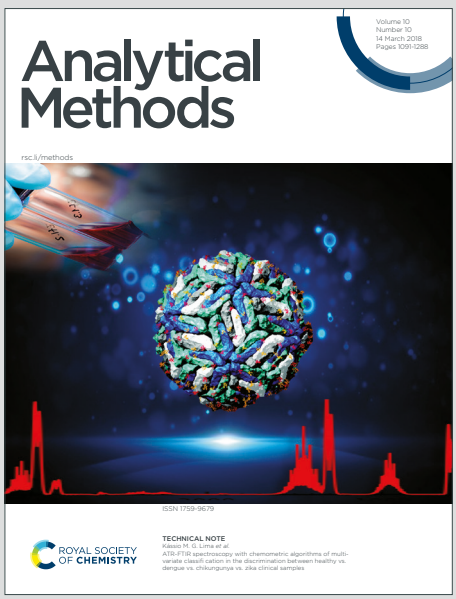

ROYAL SOCIETY OF CHEMISTRY

rsc.li/methods

Determination of Aflatoxin M1 using aptamer based biosensor on the surface of dendritic fibrous nano-silica functionalized by amine groups

Houman Kholafazad kordasht [a], Mohammad hasanzadeh [b*], Mir-Hassan Moosavy [a**], Jafar Soleymani [c], Ahad Mokhtarzadeh [e]

[a] Department of Food Hygiene and Aquatics, Faculty of Veterinary Medicine, University of Tabriz, Tabriz, Iran.

[b] Drug Applied Research Center, Tabriz University of Medical Sciences, Tabriz, Iran.

[c] Pharmaceutical Analysis Research Center, Tabriz University of Medical Sciences, Tabriz, Iran.

[d] Department of Nanochemistry, Nanotechnology Research Center, Uremia University, Uremia, Iran.

[e] Immunology Research Center, Tabriz University of Medical Sciences, Tabriz, Iran.

Corresponding Author
E-mail address: (*) hasanzadehm@tbzmed.ac.ir
(**)mhmoosavy@gmail.com

Abstract

Aflatoxins are potential food pollutants produced by fungi. One of important toxins is aflatoxin M1 (AF M1). A great deal of concern is associated with AF M1 toxicity. Aflatoxins are potential food pollutants produced by fungi. Among them, Aflatoxin M1 (AF M1) is the most toxic. A great deal of concern is associated with AF M1 toxicity. In the present work, a novel aptamer-based bioassay was developed for the monitoring of Aflatoxin M1 (AFM1) in real samples. Chitosan modified graphene quantum dot (GQDs-CS) composite was used as a biocompatible substrate to coated of dendritic fibrous nanosilica functionalized by amine groups (KCC-1-NH_2-Tb). Therefore, an innovative biocompatible polymeric matrix was prepared for the aptamer immobilization. So, unique oligonucleotide of AFM1 (5′-ATC CGT CAC ACC TGC TCT GAC GCT GGG GTC GAC CCG GAG AAA TGC ATT CCC CTG TGG TGT TGG CTC CCG TAT) labelled by toluidine blue was immobilization on the engineered interface. Hence, a novel aptamer based bioassay was formed for highly sensitive quantitation of AFM1 using cyclic voltammetry and differential plus voltammetry techniques. The structure and morphology of GQDs-CS/KCC-1-NH_2-Tb was investigated by Fourier-transform infrared spectroscopy, X-Ray Diffraction, Atomic force and Scanning Electron Microscopy and Energy-dispersive X-ray spectroscopy. The toxicity tests which performed by MTT assays, revealed the biocompatible nature of the KCC-1-NH_2-Tb. The engineered aptasensor represented excellent behaviour toward determination of AFM1 which the low limit of quantification was 10 fM. The proposed aptamer based bioassay was used for the monitoring of AFM1 in milk samples, successfully. Finally, this work provides beneficial reference for sensing of other toxins in food/pharmaceutical assays and veterinary medicine.

Keywords: DNA-aptamer, bioassay, mycotoxins, chitosan, biomedical analysis, polymeric nano-composite

View Article Online
DOI: 10.1039/C9AY01185D

Introduction

Aflatoxins are kind of fungal mycotoxins. Aflatoxin are the group of chemically diverse secondary metabolite of fungi and produced by Aspergillus numinosis, Aspergillus syodotamarty, Aspergillus nasreurosensus, Aspergillus bombasiis. [1] Among the several mycotoxins, aflatoxin B1 (AFB1) is superlative mutagenic, genotoxic and carcinogenic, furthermore Aflatoxins have four main types including: B1, B2, G1 and G2. [2] Aflatoxin M1 (AFM1) is found in milk, when cows ingested with AFB1 contaminated feed. Hence, AFM1 is the main hydroxyl metabolite of the AFB1 and have negative health implications. [3] Infected milk by AFM1 do not have any sign, such as mold and color change. [4-6]

AFM1, at first classified as a Group 2B carcinogen, [7] but now has been also reclassified in Group 1 carcinogen by the IARC (International Agency for the Research on Cancer). [8] Various methods have been designed for determination of AFM1, including thin-layer chromatography, high performance liquid chromatography (HPLC), enzyme-link immunosorbent assay and ELISA. [9] These techniques are not great like biosensors, because they have more washing steps, requiring expensive materials and equipment and also they are time consuming methods. [10]

In recent years, electrochemical biosensors for AFM1 detection have developed and which are easy to use and low cost, but the most important attributes of them is their sensitivity. [11-15] Additionally, the determination of AFM1 has been carry out via voltammetric biosensors. [13-16] A novel electrochemical biosensor based hairpin-shaped structure of AFM1 aptamer (Apt), gold nanoparticles (AuNPs) and complementary strand of the aptamer (CS) detected AFM1 with high sensitivity, selectivity and the detection limit was 0.9 ng/L. [14-17] The AFM1 monitoring by aptasensor developed based on molecular recognition element in which aptamer used via a strong interaction with biotin-streptavidin and that is complementary ssDNA. They detected AFM1up to 0.03 ng/L. [15-18] The unique platform used simple tools for determination of AFM1, which Silver nanoparticles (Ag NPs)

were electrodeposited onto green and biocompatible nanocomposite containing α-cyclodextrin a conductive matrix and graphene quantum dots (GQDs) an amplification element. [16-19]

Aptamers are short synthetic single strand DNA (ssDNA) or RNA that have high affinity when conjugated to different analyte and which are then screened with the systematic evolution of ligands by exponential enrichment (SELEX) technique. [12] In addition, aptamers basically have a length of 20-80 bases and a molecular weight of approximately 6-30 kDa. Aptamers are stable over a wide range of temperature and pH. Therefore, aptamers are reproducible. Furthermore, aptamers shows specific affinity to analytes, including proteins, amino acids, virus, low-molecular-inorganic compounds-weight organic, peptides, antibiotics, small ions and even entire cells via van der Waals forces, hydrogen bonding and electrostatic interactions. [13] Therefore, aptamers are extremely attractive molecules, which show great potential for madding vast types of biosensors (aptasensor). [14]

It is important to point out that nutraceuticals have grown in interest to researchers, industry, and consumers and are now familiar in the collective imagination as an implement for preventing the onset of a disease. Currently, nutraceuticals do not have a specific definition distinct from those of other food-derived categories, such as herbal products, food supplements, pre- and probiotics, functional foods, and fortified foods. An officially shared and accepted definition of nutraceuticals is still missing, as nutraceuticals are mostly referred to as pharma-foods, a powerful toolbox to be used beyond the diet but before the drugs to prevent and treat pathological conditions, such as in subjects who may not yet be eligible for conventional pharmaceutical therapy. Hence, it is of utmost importance to have a proper and unequivocal definition of nutraceuticals and shared regulations. It also seems wise to assess the safety, mechanism of action and efficacy of nutraceuticals with clinical data. A growing demand exists for nutraceuticals, which seem to reside in the grey area between pharmaceuticals and food. Nonetheless, given specific legislation from different countries, nutraceuticals are experiencing challenges with safety and health claim substantiation. [20,21]

View Article Online
DOI: 10.1039/C9AY01185D

Apart from the electrochemical sensing, there is some of articles related to determination of AFM1 in different samples such as milk. [22-28]

In this study, we aimed to design a novel electrochemical biosensor for the rapid and special quantification of AFM1 in milk samples. For the fabrication of this biosensor, GQD-CS and KCC-1-NH_2-Tb were synthesis and these materials electrodeposited on the surface of GCE by cyclic voltammetry (CV) and chronoamperometry (CHA) techniques. The unique oligonucleotides sequence as probe aptamer labeled by toluidine blue (TB) as an indicator was immobilized on the surface of GQDs-CS/KCC-1-NH_2-Tb. CV and differential pulse voltammetry (DPV) techniques were used for the analysis of AFM1 in real samples. To the best of our knowledge, the use of ordered GQDs-CS/KCC-1-NH_2-Tb for encapsulation of aptamer and its application to monitoring of AFM1 has not yet been reported.

Experimental details

Chemicals and reagents

All chemicals used in this research are in an analytical grade. Citric acid (glacial), sodium hydroxide (NaOH), TB, Potassium ferrocyanide $K_4Fe(CN)_6$, potassium ferricyanide $K_3Fe(CN)_6$, Mercaptoethanole (MCE), chitosan and AFM1 were procured from Sigma-Aldrich (Ontario, Canada). Acetic acid, Urea (CH_4N_2), Tetraethyl orthosilicate (TEOS), Cyclohexane, Hexanol, Cetrimonium bromide and hydrochloric acid (HCL) were procured from Merck (Germany). The oligonucleotide AFM1: 5′-ATC CGT CAC ACC TGC TCT GAC GCT GGG GTC GAC CCG GAG AAA TGC ATT CCC CTG TGG TGT TGG CTC CCG TAT sequence was obtained from Takapouzist Co. A stock of solution of 20 µM TB was prepared in Tris-HCl buffer 0.1 M and was use as redox indicator for ascertain oligonucleotide hybridization. The standard AFM1 solutions was prepared by Tris-HCl buffer 0.1 M and that solution was diluted by Tris-HCl buffer 0.1 M. All the above solutions were kept at -4 ◦C before use. Ferrocyanide/ ferricyanide solution containing 0.5 M of $K_4Fe(CN)_6$/$K_3Fe(CN)_6$ and 0.5 M KCl (1:1) were prepared to the electrochemical measurement of the microscopic surface

areas of the working electrodes. All the above solutions were kept at -4 ◦C before use. The pasteurized milks was prepare from hyper markets and the raw milk from local store.

Apparatuses and methods

Electrochemical measurements for cyclic CV, CHA and DPV were carry out with a computer controlled AUTOLAB system with PGSTAT 302N (Eco Chemie, Utrecht, The Netherlands), driven with NOVA 1.11 software. Ordinary 3-electrode was operated a reference electrode by an Ag/AgCl (Methrom, The Netherlands) and a platinum wire was utilize as a counter electrode and GCE as a working electrode (d = 2 mm) (from Azar electrode Co, Iran). The surface morphology of electrode was evaluated by high-resolution field emission scanning electron microscope (FE-SEM, Hitachi-SU8020, Czech) and chemical compositions of the electrode were analyzed by an EDS or EDX coupled with the FE-SEM equipment. TEM analysis was conducted on a Philips CM30 electron microscope (Adelaide, Australia). DLS was analyzed with zeta potential instrument Malvern Instruments Ltd (Zetasizer Ver. 7.11, MAL1032660, England) for zeta potential and size distribution of Tb-KCC-1-NH_2, GQDs and GQDs-CS nanocomposites. The phase purity was examined by XRD using a Rigaku D/max 2500 diffractometer and FT-IR spectra (4000-400 cm^{-1}) were recorded with a Shimadzu FT-IR Prestige 21 spectrophotometer as KBr disks. The AFM images were recorded on Bruker Dimension Icon microscope in ScanAsyst regime with OTESPA AFM probes (Bruker) and TEM images were obtained by TEM, Leo 906,100 kV, Zeiss (Germany). BET method were distinguished via nitrogen-desorption isotherms using Belsorp-mini II analyzer (MicrotracBEL, Japan).

Synthesis and characterization of the materials

GQDs and GQDs-CS synthesis and characterization

GQDs and GQDs-CS were synthesized according to our previous work [19]. An easy bottom-up method was used for the preparation of GQDs. At first, GQDs were synthesized by pyrolyzing citric acid and dispersing the carbonized products into alkaline solutions. Briefly, 2 g of citric acid was put into a beaker and heated to 200 °C by a heating mantle until the citric acid changed to an orange liquid. Then, for preparing GQDs, 100 mL of 10 mg/mL NaOH solution was added into the orange homogenous liquid dropwise with continuous stirring. The obtained GQD solution was stable for at least one month at 4 °C and in GQDs-CS synthesis, CS solution (2 g. L^{-1}) was prepared by dissolving CS in 0.1 M acetic acid, and then the yellow GQDs aqueous solution (2 g. L^{-1}) was added into the CS solution under stirring. After 10 min of stirring, the mixture was adjust by addition of 10% (w/w) sodium hydroxide solution dropwise. The precipitate was washed with ultrapure water several times to remove the residual impurities, and the obtained GQDs-CS were freeze dried in a lyophilizer at -40 ◦C for 24 h. The GQDs toxicity was evaluated in previous research on NIH-3T3 and HepG2 cells, so these cell exposed to different concentrations of GQD (0, 10, 20, 50,100 and 200 ppm) for 24, 48 and 72 hour (Mirzaie et al., 2019). As a result increasing doses of GQD up to 200 ppm, do not have any striking result on cell viability by MTT.

FT-IR, DLS, Zeta potential analysis, XRD and AFM were used for the characterization of GQD and GQDs-CS nanocomposites. By FT-IR, the surface chemistry of GQDs and CS-GQDs were investigated. The FT-IR spectrum of GQDs and GQDs-CS nanocomposites are shown in (Fig. S1A) and that spectrum about GQDs showed two main peaks at 1716 $cm^{-1}$and 1766 cm^{-1} and these are assigned to the stretching vibrations of C=O from the −COOH groups. For GQDs-CS, two peaks at 1604 and 1766 cm^{-1} are related to strong electrostatic attraction between CS and GQDs. Furthermore the C=O stretching of GQDs is reduce from 1716 to 1708 cm^{-1}, which can be Arising from the formation of H-bending inside the nanocomposites.

The DLS study result showed a growth in the particle size of the GQDs-CS that accepted via zeta potential analyses (Fig. S1B).The result show that CS was successfully attahed to GQDs structure,

which caused to negative zeta potential value was changed to more negative potentials and where the negative charge have a major effect in stability of GQDs-CS (Fig. S1C).

XRD template were checked on a Siemens D 5000 X-Ray diffractometer (Texas, USA) with a Cu Kα anode (λ = 1.54 A°) operating at 40 kV and 30 mA. The diffraction patterns were collected at 25 °C and over an angular range of 3.0 to 10 and 10 to 70° with a dwell time of 12 s per increment and step size of 0.05° per step (Fig. S1D). For more confirmation, the morphology of GQDs and GQDs-CS were characterized by AFM image (Fig. 1E).

Synthesis and characterization of KCC-1-NH_2-Tb

The KCC-1 synthesis follow a generic synthesis (Polshettiwar et al., 2010. Briefly, tetraethyl orthosilicate (TEOS, 2.5 g, 0.012 mol) was dissolved in a solution of cyclohexane (30 mL) and pentanol (1.5 mL) and then a stirred solution of cetylpyridinium bromide (CPB; 1 g, 0.0026 mol) and urea (0.6 g, 0.01 mol) in water (30 mL) was then added. Fig. S2A is TEM images of KCC-1 and that is confirmed successful synthesis of this material. For the synthesis of KCC-1-NH_2, 20 ml THF and 2 mmol of KCC-1 were combine together and the next 20 mmol of NaOH was dispersed in to the mixture by sonication (Sadeghzadeh et al., 2018). 22 mmol of 3-aminopropyltriethoxysilane (APTES) was added drop by drop at room temperature and stirred for another 16 h at 60 °C. The acquired obtained products were collected and washed with deionized water and ethanol in sequence and afterward dried action has done under vacuum at 60 °C for 2 h for further use. Scheme 1 was summarized all of the synthesis procedure. The TEM images of KCC-1-NH_2 has showed in (Fig. S2B). For the KCC-1-NH_2-Tb synthesis 1 g CTAB, 225 g water and 3.5 ml NaOH were mixed together. Then 55.5 ml TOES and 15 ml of Tb^{+3} were added. The mixture was incubated at 20 ° C for 2 h. then the composite washed with ethanol and water. The drying process was done at the room temperate in the vacuum (See Scheme S1 in supporting information). The comparison TEM images of the KCC-1 and KCC-1-NH_2 show that the structure is similar, but the KCC-1-NH_2-Tb morphology is amorphous (Fig. S2). On the other hand, investigated of the agglomeration and local accumulation only indicate low agglomeration

of KCC-1-NH_2-Tb. According to Fig. S4, the structure form of these compounds are dendrite spheres with uniform structure. The images clearly illustrated that these materials possesses dendrite fibers orderly in three dimensions to form spheres, which may let effortless access to the available high surface area.

The XRD analysis (Fig. S5) demonstrate two peak centered at around 11θ and 22 θ in both KCC-1 and KCC-1-NH_2, respectively. Also KCC-1-NH_2-Tb has wide peak centered at around 22 θ.

The specific surface area and porosity of the materials were determined using the adsorption isotherm and calculated by BET. Also, BJH method was used to determine the pore volume of the KCC-1, KCC-1-NH_2 and KCC-1-NH_2-Tb. Table S1 lists the average pore size, surface area and pore volume of KCC-1, KCC-1-NH_2 and KCC-1-NH_2-FA. The BJH pore volumes were changed from 1.52 to 1.1 and 1.01 cm^3/g for KCC-1, KCC-1-NH_2 and KCC-1-NH_2- Tb and surface area of KCC-1 changed from 617 m^2/g to 367 and 633 m^2/g for KCC-1-NH_2 and KCC-1-NH_2-Tb, respectively. Mean pore diameter distribution of the materials were 9.9, 11.9 and 6.94 for KCC-1, KCC-1-NH_2 and KCC-1-NH_2-FA, respectively (Fig. S6). The pore size, pore volumes and surface area of KCC-1, KCC-1-NH_2 and KCC-1-NH_2-Tb are obviously confirmed by the previously reported results.

Functional groups of the synthesized materials was characterized by FTIR. As shown in Fig. S7, the characteristic peaks of the silica based materials could be observed in the range of 1020 to 1110 cm^{-1} representing the Si-O-Si asymmetric stretching and Si-OH peak is observed at 960 cm^{-1} which represents the stretching vibration and asymmetric bending. Also, the peak at around 1500 cm^{-1} is assigned to the Tb and KCC-1-NH_2.

The DLS study indicated that particle size of KCC-1-NH_2 was increased, but the KCC-1-NH_2-Tb particle size is almost similar (Fig. S8). The toxicity of KCC-1-NH_2-Tb was investigated by MTT assay on HT 29 cancer cell lines in the different concentration (1, 10, 20, 50, 100 and 150 ppm) for 24, 48 and 72 h. The result show that the KCC-1-NH_2-Tb is not toxicity material (Fig. S9).

Electrodeposion of GQDs-CS and KCC-1-NH_2-Tb

Before start experiment, the GCE was polished for having reliable and repeatable responses. In this regard, polishing was done with 0.05 µm alumina (Beuhler, USA) powder on the standard pad, afterward the GCE was ultrasonically rinsed steadily with 1:1 alcohol, acid nitric and water. Finally it allowed to dry at room temperature (Engstrom et al., 1982). Covering of GCE surface is extremely momentous step in the design of the biosensor. For this purpose, electrochemical deposition of GQDs-CS on the surface of GCE was done and that show in (Fig. S10.A). The electrochemical deposition was started, when GCE located in in the cell containing 10 mL of CS-GQDs and that procedure was manufactured via CV with 30 consecutive cycles in the potential range of 0 to 1 V *vs.* Ag/AgCl. Also, $-NH_2$ groups of CS at the C-2 position of the D-glucopyranose repeating unit could be protonated in the acidic media. [27, 28] On the other hand, the result of GQDs dispersed in water has extremely negative charge. So ionization of oxygen containing functional groups (mainly−COOH) on the structure of GQDs, which is favor of their composition with positively charged CS. In addition, the zeta potentials result, prove GQDs have negatively charged (−10 mV) and CS with NH^{3+} groups is positively charged (+65 mV). The $-NH^{3+}$ groups on CS chip has electrostatic attraction with dominant −COO− groups of GQDs. Hence, there also exist vast H-bindings between−OH groups on the surface of GQDs and $-CO_2H$ groups of CS. H- bonding and both electrostatic attraction persuade interfacial adhesion of GQDs and CS, lead to formation of homogeneous nanocomposites of GQDs-CS. At the second step, KCC-1-NH_2-Tb was electrodeposited on the surface of GQDs-CS using CHA techniques at the E=-0.24V and duration time of 500 s (Fig. S10.B). KCC-1-NH_2-Tb have negative.

Immobilization of aptamer

In generally immobilization of aptamer on the surface of CS-GQDs/KCC-1-NH_2-Tb was done and then all of electrodes were rinse with deionized water. So, drying at the room temperature was performed. For the immobilization of aptamer, 5 µL of primary DNA aptamer (5′-ATC CGT CAC ACC TGC TCT GAC GCT GGG GTC GAC CCG GAG AAA TGC ATT CCC CTG TGG TGT TGG CTC CCG TAT) was diluted by 500 µL Tric-HCl buffer and mixed with 5 µL of that dilution with 5

µL of TB (20 µM) which is indicator. So the designed substrate (CS-GQDs/KCC-1-NH_2-Tb) was incubated with primary aptamer at -4 °C for 6 h. Then, MCE as blocking reagent was added to the surface of the modified electrode to reduce non-specific adsorption for 20 min (Scheme 1).

Characterization of electrode surface

In Fig. 1, the morphology of the engineered electrode surface and monitoring the distribution were investigated carefully. The result reveled that, slim layer of GQDs-CS was covered on the GCE (Fig. 1A). Fig. 1B exposing that the KCC-1-NH_2-Tb were indeed bounded and assembled onto the surface of GQDs-CS. Aptamers were successfully immobilization on surface of KCC-1-NH_2-Tb. The FE-SEM images prove fabricate is correct (Fig. 1C).

All the data has proven by EDX, because compared KCC-1 and KCC-1-NH_2 diagram show that Si, N, O and C element peaks increased. The comparison of KCC-1-NH_2-Tb diagram with two previous diagram show the Terbium elements were found to accumulate in between of KCC-1.

Results and discussion

Electrochemical behaviour

Fig. 2.A revealed CVs of GCE modified by GQDs-CS, KCC-1-NH_2-Tb and GQDs-CS/KCC-1-NH_2-Tb in the absence of AFM1 at a potential range of -1 to +1 V and a scan rate of 100 mV/s. It should be noted these electrode were assessed in the Ferrocyanide/ ferricyanide as mediator. As can be seen, after the GCE modified by GQDs-CS, the peak current was increase and that electrode have higher oxidation peak current than other electrode. When the GCE modified by KCC-1-NH_2-Tb the peak current was decrease and that electrode have lower oxidation peak current. Because of the high-surface area of the KCC-1-NH_2-Tb [3S], the GCE modified by GQDs-CS/KCC-1-NH_2-Tb. Peak potential was changed almost to the negative potential. The Fig. 2 revealed that the peak current of GQDs-CS/KCC-1-NH_2-Tb is average of GQDs-CS and KCC-1-NH_2-Tb. So combination of GQDs-CS and KCC-1-NH_2-Tb significantly improves interface for dense loading of aptamer. At the end time, The AFM1 behavior was investigated at the two different time (15 min and 45 min). The incubated

for 15 min have higher peak current in 45 min. The result in the Fig. 2B indicated that, the optimum incubation time is 15 min.

Assessment stability

For check the performance of biosensor, stability is important factor. Fig 3 shows CVs of GCE modified by GQDs-CS/KCC-1-NH_2-Tb in different cycle number. As can be seen, with increase of the cycle numbers to 100, peak current was not changed, which confirmed high stability of the interface.

Analytical approach

DPV is the ultrasensitive electrochemical technique for the targeting of analytes. DPV have several benefits such as less background current, better resolution and have much higher current sensitivity in comparison to CV. This benefits caused to this technique can evaluated the analytical performance of the designed aptasensor for the detection of AFM1 in the standard and milk samples. Fig. 4A display DPV response and calibration curves of the GQDs-CS/KCC-1-NH_2-Tb/aptamer in different concentration of AFM1 in standard sample. A well-defined oxidation peak were appeared by DPV. Furthermore, an excellent linear relationship between the peak currents and AFM1 concentration was obtained. The peak currents were symmetric to AFM1 concentration in the range of 0.1 μM-1 fM. Also, LLOQ was measure to be 10 fM for this analyte. The low detection limit of the engineered aptasensor is related to high surface area of the KCC-1-NH_2-Tb and sensitivity of the aptamer. Fig. 4 (B and C) showed DPV response and calibration curves of the GQDs-CS/KCC-1-NH_2-Tb/aptamer in different concentration of AFM1 in pasteurized milk and local milk, respectively. Obtained result showed that in the all three curves, with decrease of concentration of the AFM1, the peak current was increase.

DPV technique applied for evaluate the response of the proposed aptasensor towards scrineeng of AFM1 in milk samples (Fig. 4). For this purpose, different concentration of the AFM1 (0.1 μM to 1 fM) were added to the milk samples and DPVs were recorded. As shown in Fig. 4, an appropriate

View Article Online
DOI: 10.1039/C9AY01185D

linear relationship between the current response signal and the AFM1 concentrations was achieved in the range of 0.1 μM- 1 fM. As can be seen in the Fig. 4 (A-C), with decrease of the concentration, the peak current was increase. The regression of the standard sample, pasteurized milk and local milk are y = 5.315x + 26.942, y = 4.8666x + 13.35 and y = 8.0973x - 8.5695, respectively.

Finally, obtained results were compare with the previously developed aptasensors (Table 1) and previous methods (Table 2). It is clear to our proposed method has better response to other developed methods or aptasensors. Therefore, engineered aptasensor can be used as an excellent aflasensor. Also, this aptasensor can be applied in food control as a new biodevice [].

Long term stability of aptasensor

Inter-day and intra-day assessment were performed using from FDA validation standard to demonstrate the correctness of the reported method. According to obtained result proposed aptasensor is stabile till two days (Fig. 5A). Finally, repeatability of the aptasensor was studied by three electrode which similar results were obtained (Fig. 5B).

Apart from the electrochemical sensing, the change of fluorescence intensity of biomolecules for sensing and imaging should be another important and interest tool. For example, the dyes with aggregation-induced emission (AIE) feature have been extensively utilized for sensing and biological imaging applications [56-68].

Conclusion

In the summary, we developed a novel electrochemical interface engineered by GQDs-CS (as conductive layer), KCC-1-NH_2-Tb (as a high surface element) and specific aptamer for the detection of AFM1. Then unique oligonucleotide was immobilization on the surface of the engineered electrode. The results obtained by DPV technique show that this GQDs-CS/KCC-1-NH_2 is a great interface for aptamer immobilization and ultrasensitive detection of AFM1 in milk samples. Based on the DPVs and calibration curves this labeled aptasensor (GQDs-CS/KCC-1-NH_2-Tb-Aptamer labeled by toluidine blue) is appropriated or the monitoring of AFM1 in the linear rage of 0.1μM- 1fM. The

LLOQ of the developed aptasensor is 10 fM. Obtained results show that proposed aptasensor is stable till two days and GQDs-CS/KCC-1-NH_2 was not change with increased number of cycle to 100. Finally, this high selectivity, rapid and accurate apta-assay was used for the detection of AFM1 in milk samples which is important in food control.

Acknowledgments

Research was support by Tabriz University and Tabriz University of Medical Sciences. This report is part of MSc thesis of H. Kholafazad kordasht.

Conflicts of interest

No potential conflict of interest was reported by the authors.

References

[1] EE. Crepp, *Toxicol Lett.* 2002, **127**, 19-28.

[2] C. Antonio, L. Cavalheiro, *World's Poultry Science Journal in New Zealand*, 1981, **37**, 34-38

[3] A. Prandini, Tansini, G., Sigolo, S., Filippi, L., Laporta, M., & Piva, G. *Food Chem. Tox.* 2009, **47**, 984e991.

[4] CG. Cathey, Huang ZG, Sarr AB, Clement BA, Phillips TD. *J Dairy Sci.* 1994, **77**, 1223-1231.

[5] HP. Van Egmond. Introduction to Mycotoxins in Dairy Products. 11 London, UK: Applied Science Publishers; 1989.

[6] R.S. Applebaum, RE. Brackett, DW. Wiseman, EH. Marth. *J Food Prot.* 1982, **45**, 752-777.

[7] International Agency for Research on Cancer. Some Naturally Occurring Substances: Food Items and Constituent Heterocyclic Aromatic Amines and Mycotoxins. Lyon, France: IARC; 1993.

[8] International Agency for Research on Cancer (IARC). Some traditional herbal medicines, some mycotoxins, naphthalene and styrene. IARC Monographs on the Evaluation of Carcinogenic Risks to Humans. 2002, **82**, 171–6.

[9] L. Shundo, M. Sabino *J. Microbiol*. 2006, **37**, 164-170.

[10] YC. Lim, AZ. Kouzani, W. Duan, *J. Biomed. Nanotech.* 2010, **6**, 93-105

[11] A. Sassolas, L.J. Blum, B.D. Leca-Bouvier, *Biotech. Adv.* 2012, **30**, 489-571.

[12] M. Ilgu, M. Nilsen-Hamilton, *Analyst* 2016, **141**, 1551-1568.

[13] H. Malekzad, A. Jouyban, M. Hasanzadeh, N. Shadjou, M. de la Guardia, *Trends Anal. Chem,* 2017, **94**, 77-94.

[14] M. Citartan, S.C. Gopinath, J. Tominaga, *Biosens. Bioelectron.* 2012, **34**, 1–11.

[15] A. Afkhami, P. Hashemi, H. Bagheri, J. Salimian, A. Ahmadi, T. Madrakian. *Biosens. Bioelectron* 2017, **93**, 124-131

[16] A. Karczmarczyk, AJ. Baeumner, KH. Feller, *Electrochim. Acta*. 2017, **243**, 82-89.

[17] SH. Jalalian, M. Ramezani, NM. Danesh, NM. Danesh, M. Alibolandi, K. Abous, SM. Taghdisi. *Biosens. Bioelectron*, 2018, **117**, 487-492

[18] X. Guo, F. Wen, N. Zheng, S. Li, ML. Fauconnier, J. Wang. *Analytical and Bioanalytical Chemistry,* 2016, **408**, 5577-5584

[19] R. Shadjou, M. Hasanzadeh, M. Heidar-poor, N. Shadjou. *J. Molecul. Recognition,* 2018, **31**, 1-9.

[20] A. Santini, S.M. Cammarata, G.Capone, A.Ianaro, G.C. Tenore, L. Pani, E. Novellino. *Br. J. Clin. Pharmacol.* 2018, **84**, 659-672.

[21] P. Daliu, A. Santini, E. Novellino. *Expert Opin Ther Pat.* 2018, 28, 875-882.

[22] A. Santini, A. Raiola, V. Ferrantelli, G. Giangrosso, A. Macaluso, M. Bognanno, F. Galvano, A. Ritieni. *Food Additives Contaminants: Part B: Surveillance.* 2013, **6**, 181-186.

[23] O. Ketney, A. Santini, S. Oancea. *International J. Dairy Tech*, 2017, **70**, 1-12.

[24] A. Santini, A. Ritieni. Aflatoxins: Risk, Exposure and Remediation. Chapter 16. In Aflatoxins - Recent Advances and Future Prospects. *Intech*. 2013, http://dx.doi.org/10.5772/52866.

[25] P. Mikušová, A. Šrobárová, M. Sulyok, A. Santini. *Mycotoxin Research,* 2013, **29**, 97-102.

[26] P. Mikusova, A. Ritieni, A. Santini, G. Juhasova, A. Srobarova. Food Additives Contamin, *Part A: Chem., Anal, Control, Exposure Risk Assessment.* 2010, **27**, 738-747.

[27] A. Santini, R. Ferracane, G. Meca, A. Ritieni, Overview of analytical methods for beauvericin and fusaproliferin in food matrices. *Anal. Bioanal. Chem.* 395, 2009, 1253-1258.

[28] A. Santini, G. Meca, A. Ritieni. *World Mycotoxin J.* 2012, **5**, 71-81

[29] S. H. Jalalian, M. Ramezani, N.M. Danesh, M. Alibolandi, K. Abnous, S. M. Taghdisi. *Biosens. Bioelectron.* 2018, **117**, 487-492.

[30] G. Istamboulié, N. Paniel, L. Zara, L.R. Granados, L. Barthelmebs, T. Noguer. *Talanta* 2016, **146**, 464-469.

[31] B.H. Nguyen, L.D. Tran, Q.P. Do, H.L. Nguyen, N.H. Tran, P. Nguyen. *Mater. Sci. Engin.: C.* 2013, **33**, 2229-2234

[32] S.C. Pei, Y.Y. Zhang, S.A. Eremin, W.J. Lee, *Food control.* 2009, **20**, 1080-1085

[33] J. Wang, B. Liu, Y. Hsu, F. Yu. *Food Control*, 2011, **22**, 964-969

[34] H Tajik, MR Rohani, M Moradi. *Pakistan J. Biolo.* 2007, **10**, 4103-4107.

[35] L. Micheli, R. Grecco, M. Badea, D. Moscone, G. Palleschi, *Biosens. Bioelectron*, 2005, **21**, 588-596.

View Article Online
DOI: 10.1039/C9AY01185D

[36] A. Vig, A. Radoi, X. Muñoz-Berbel, G. Gyemant, J.-L. Marty, *Sens. Actuators B Chem*. 2009, **138**, 214-220.

[37] D. Neagu, S. Perrino, L. Micheli, G. Palleschi, D. Moscone, *Int. Dairy J.* 2009, **19**, 753–758.

[38] E. Larou, I. Yiakoumettis , G. Kaltsas, A. Petropoulos, P. Skandamis, S. Kintzios, *Food control*. 2013, **29**, 208-212.

[39] E.K. Kim, D. H. Shon, D. Ryu, J. W. Park, H. J. Hwang & Y. B. Kim. *Journal of Food Additives and Contaminants*. 2000, **17**, 59-64.

[40] Y. Wang, X. Liu, C. Xiao, Z. Wang, J. Wang, H. Xiao, L. Cui, Q. Xiang, T. Yue. *Food Control.* 2012, **28**, 131-134.

View Article Online
DOI: 10.1039/C9AY01185D

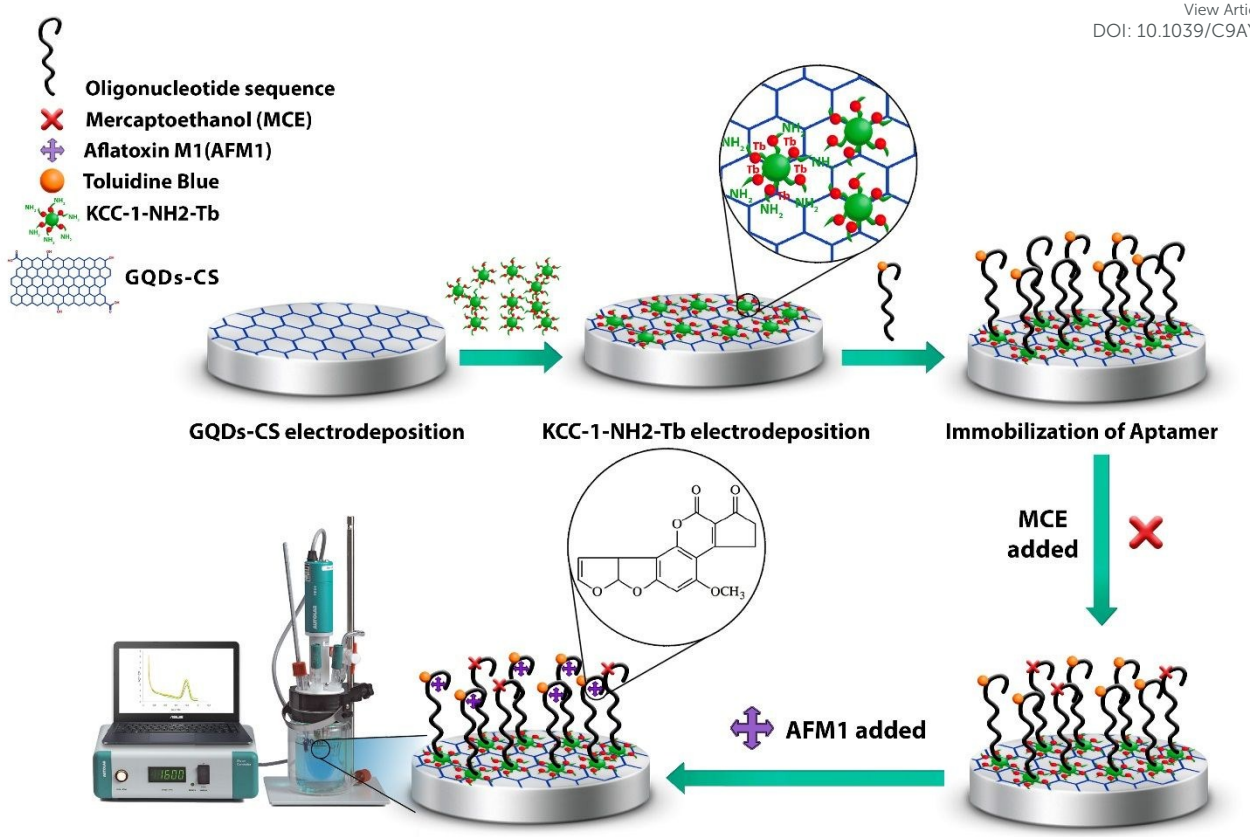

Scheme 1: Aptasensor assembly procedure and its application to monitoring of AF M1.

View Article Online
DOI: 10.1039/C9AY01185D

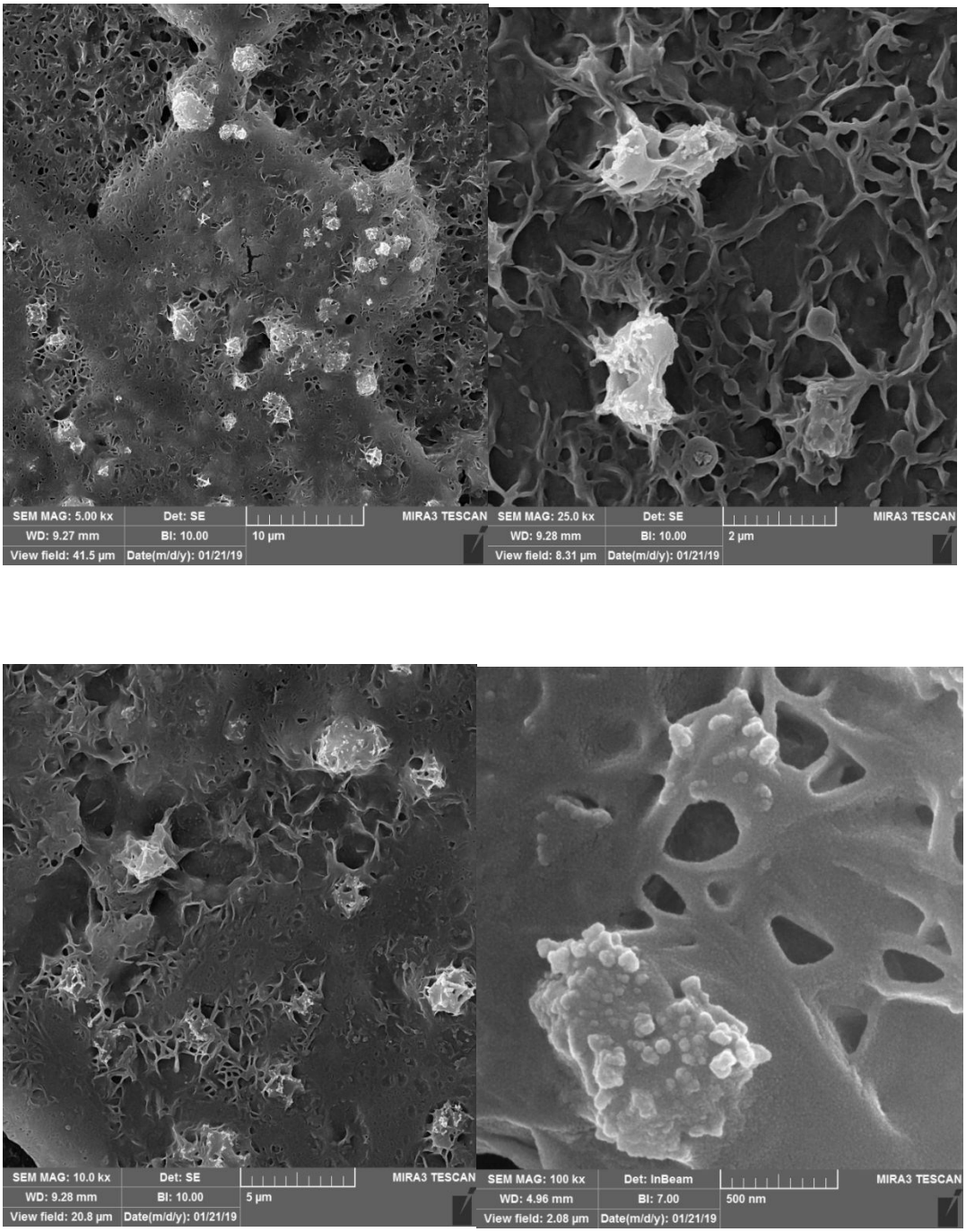

Fig. 1A

View Article Online
DOI: 10.1039/C9AY01185D

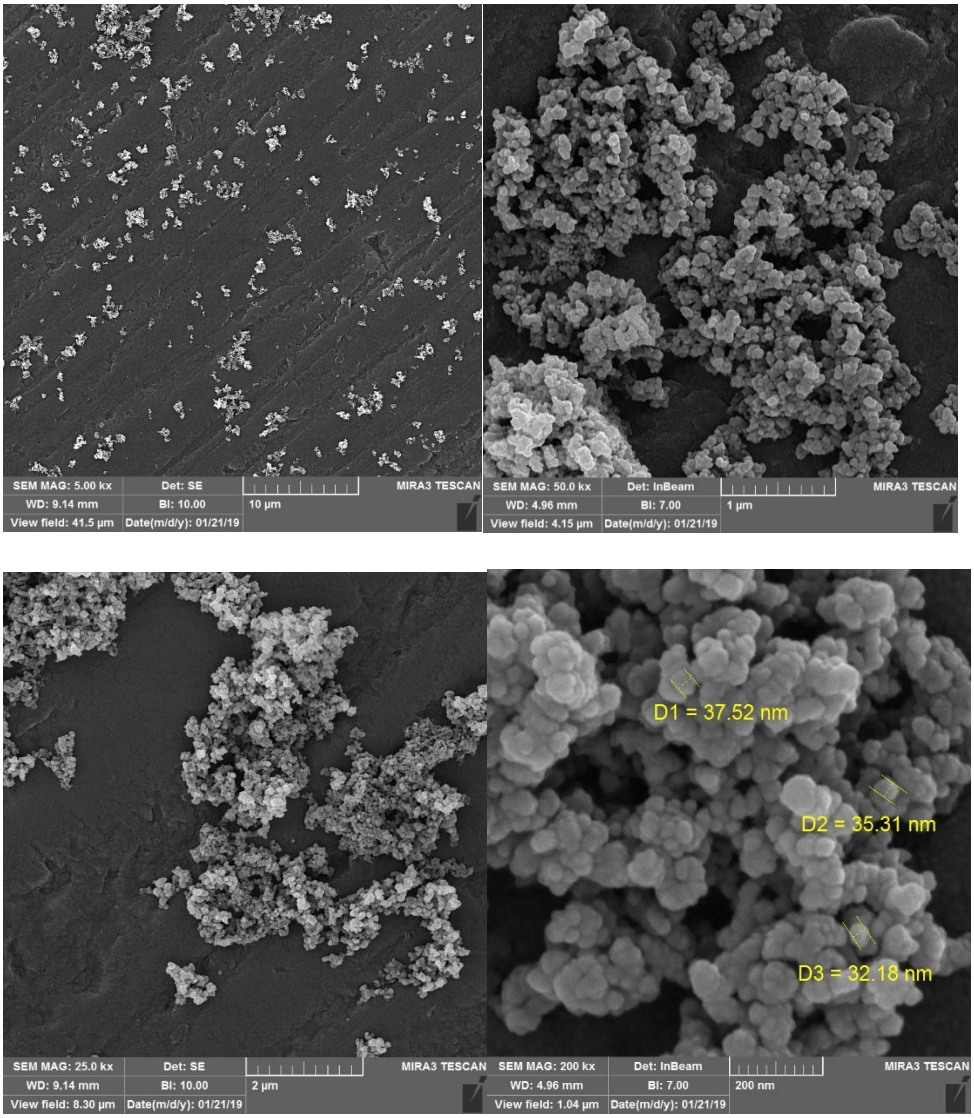

Fig. 1B

View Article Online
DOI: 10.1039/C9AY01185D

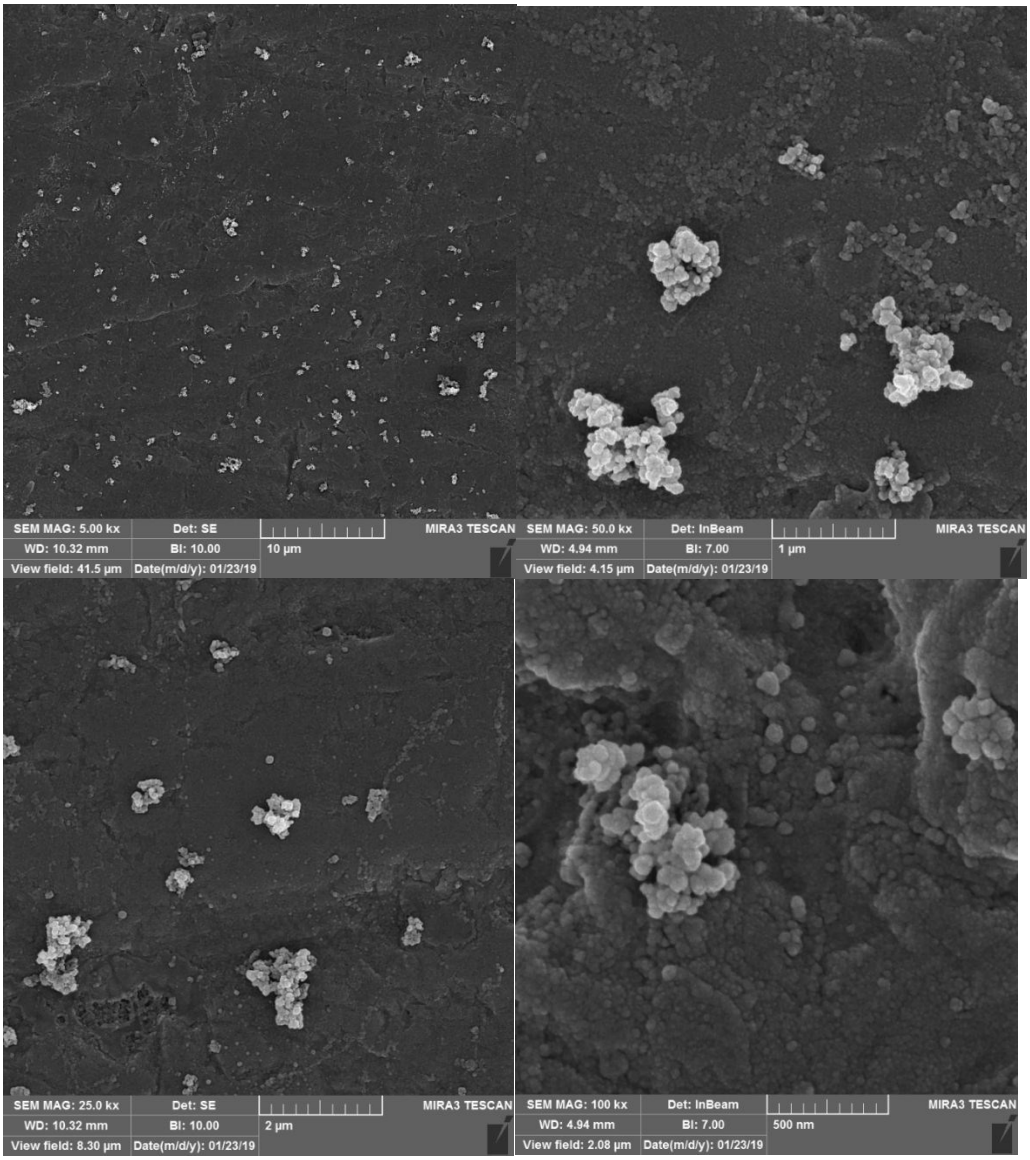

Fig. 1C

Fig. 1. FE-SEM images of the GQDs-CS/GCE (A), GQDs-CS/KCC-1-NH_2-Tb/GCE (B) and GQDs-CS/KCc-1-NH_2-Tb/Aptamer/GCE (C) in different magnification.

View Article Online
DOI: 10.1039/C9AY01185D

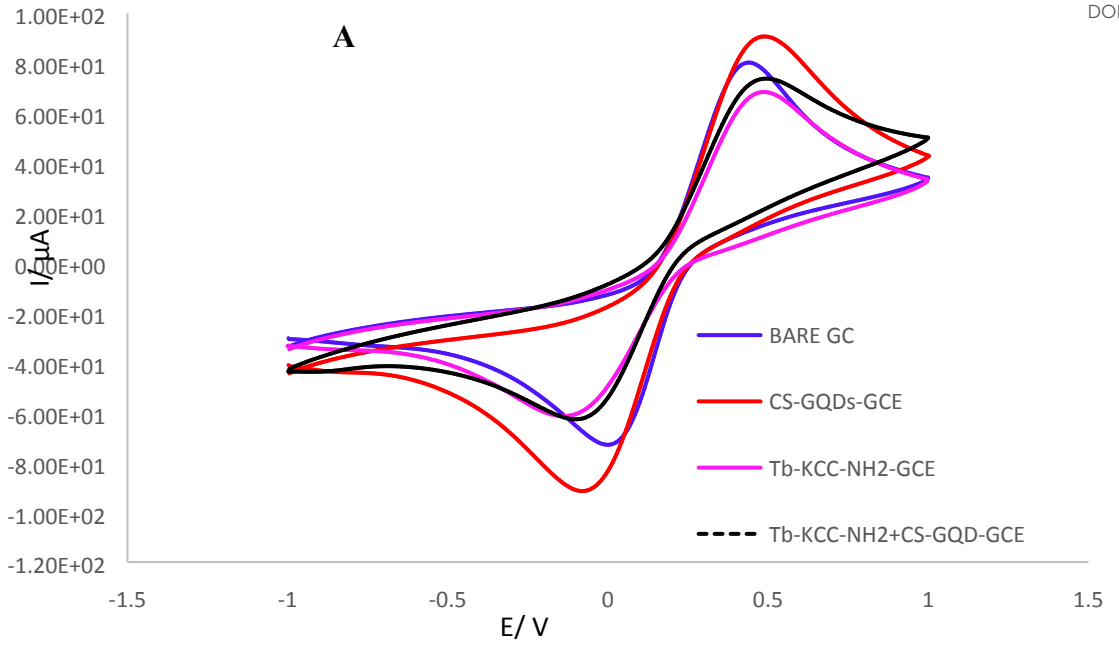

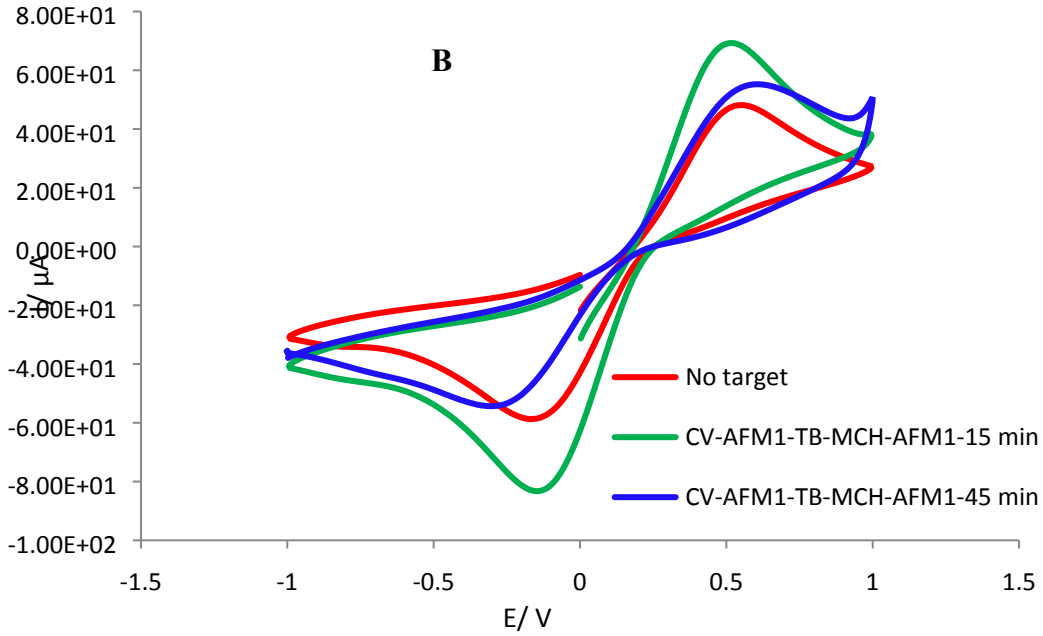

Fig.2: **A)** CVs of GCE, GCE modified by GQDs-CS, KCC-1-NH_2-Tb and GQDs-CS/KCC-1-NH_2-Tb in the -1 to +1 potential V , **B)** and the AFM1 behavior in Ferrocyanide/ ferricyanide solution at the two different time.

View Article Online
DOI: 10.1039/C9AY01185D

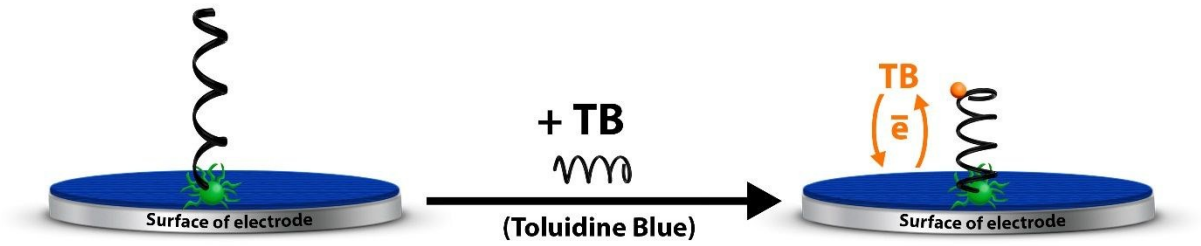

Scheme 2: Detection procedure of AM1 using proposed aptasensor.

View Article Online
DOI: 10.1039/C9AY01185D

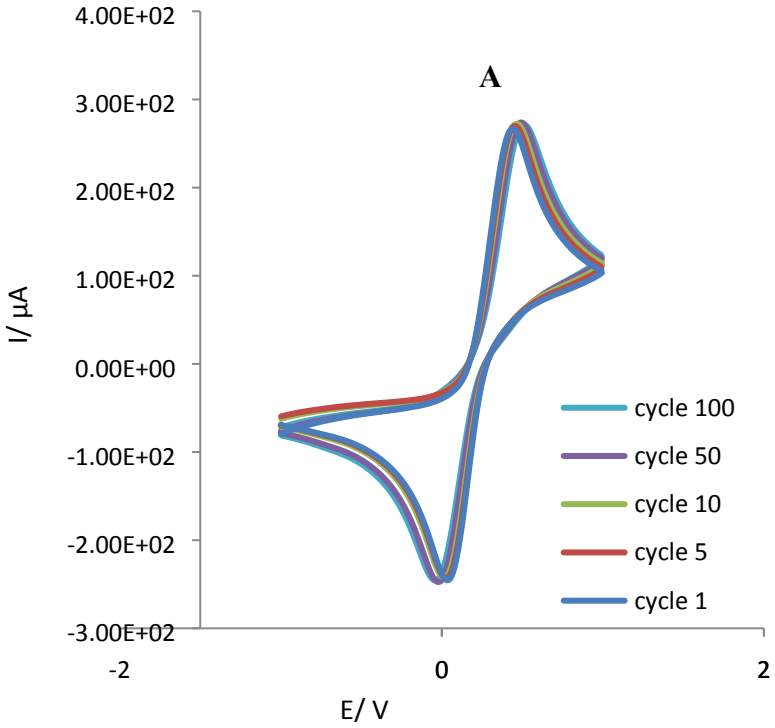

Fig.3: CVs of GQDs-CS/KCC-1-NH_2-Tb in different cycle number.

View Article Online
DOI: 10.1039/C9AY01185D

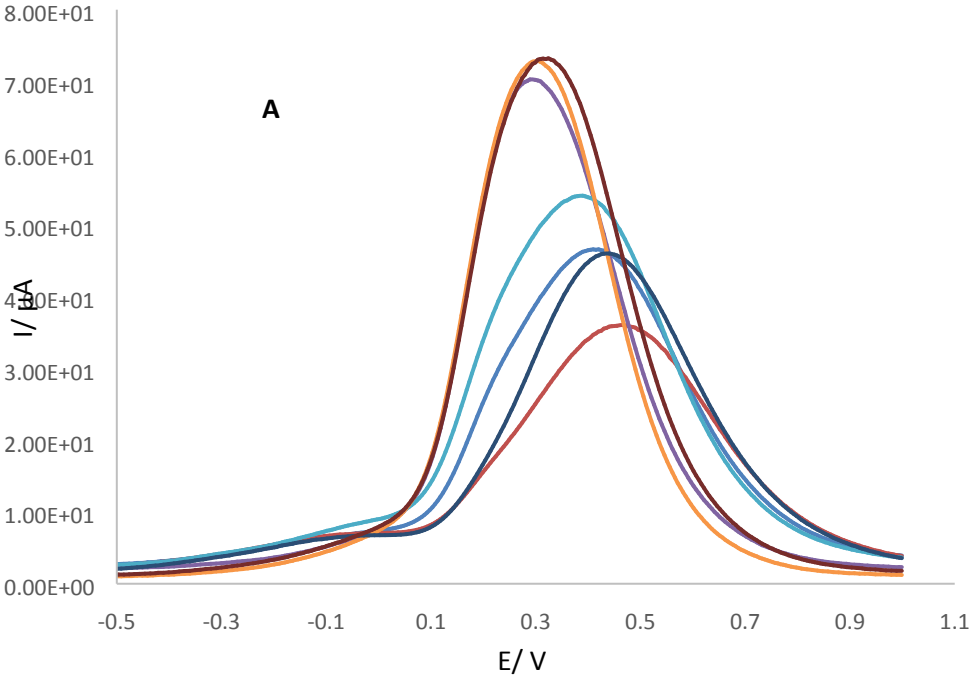

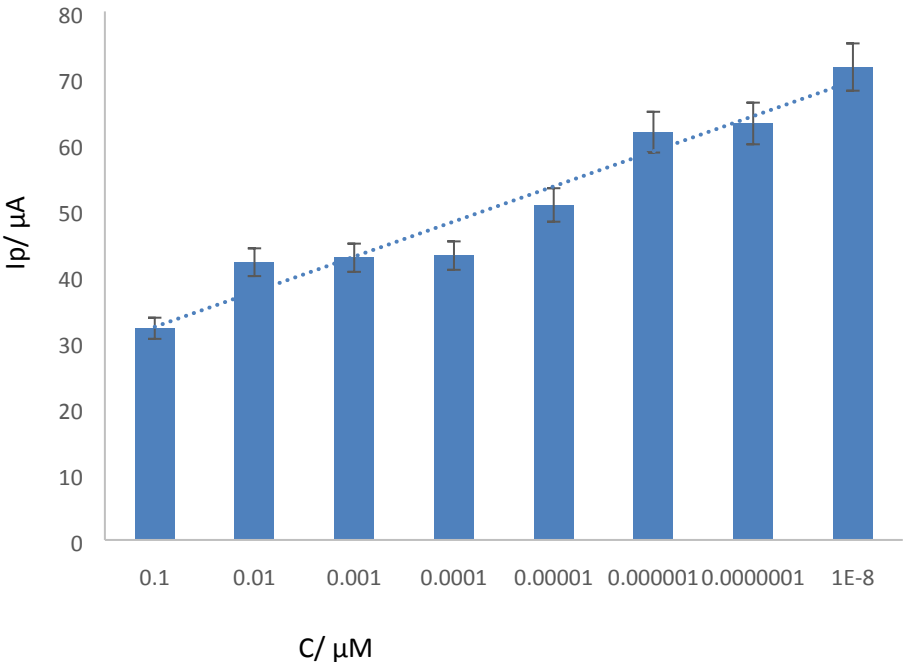

View Article Online
DOI: 10.1039/C9AY01185D

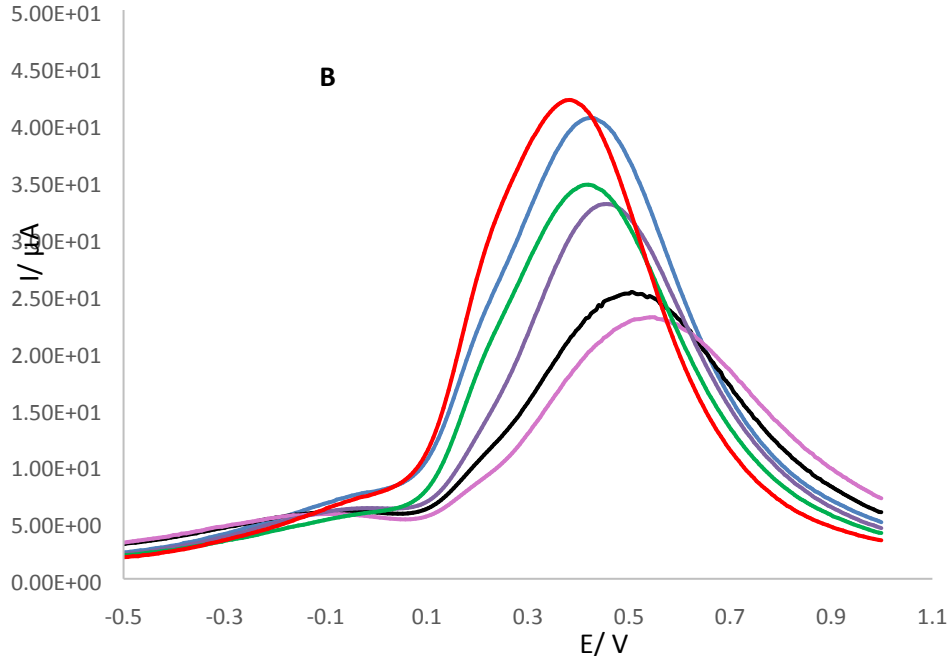

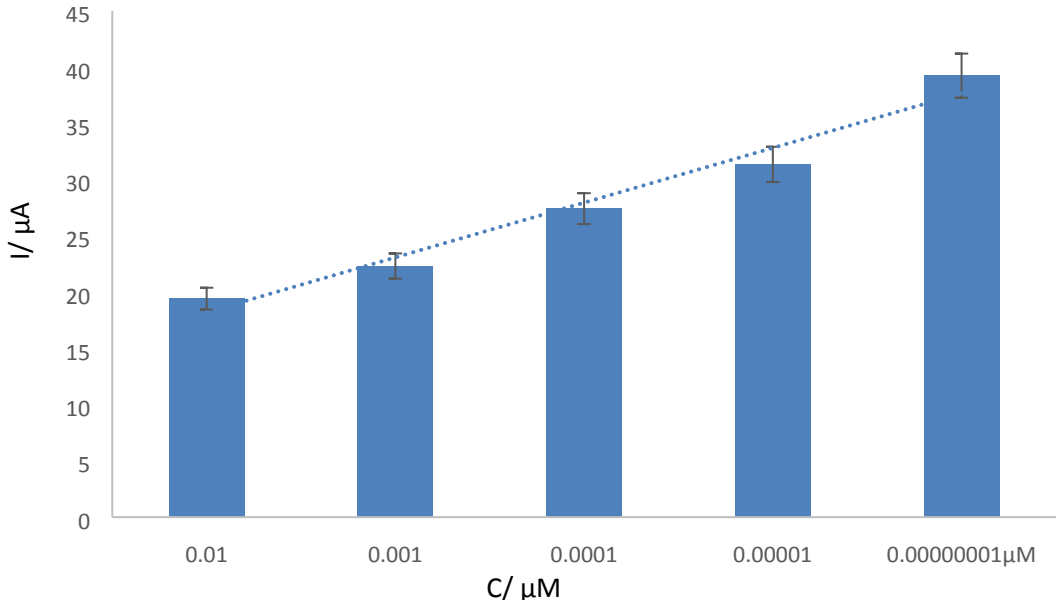

View Article Online
DOI: 10.1039/C9AY01185D

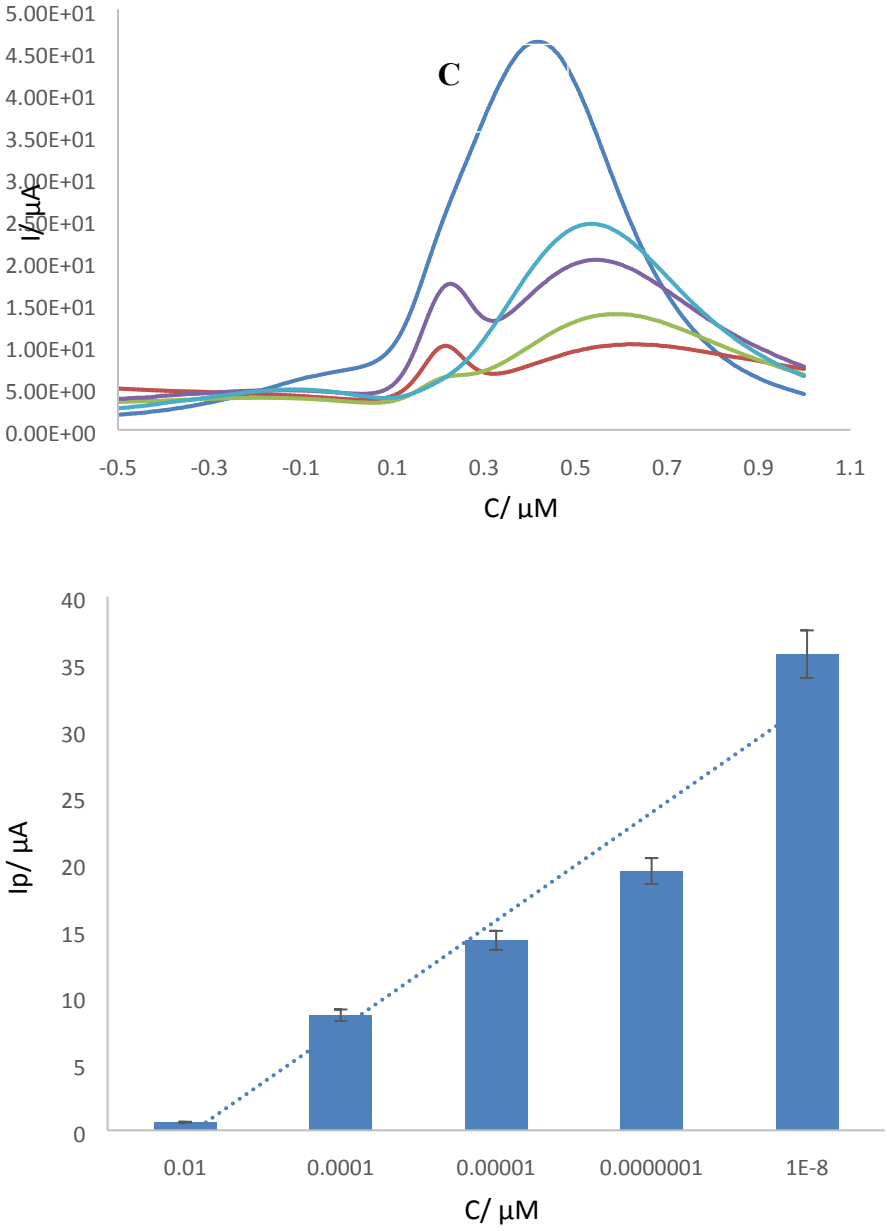

Fig. 4. DPVs of the GQDs-CS/KCC-1-NH_2-Tb/Aptamer in the presence of AF M1 with different concentration (0.1 µM, 0.01 µM, 0.001 µM, 0.0001 µM, 0.00001 µM, 0.000001 µM, 0.0000001 µM and 0.00000001 µM) of Aflatoxin M1 (AFM1) in the Tric-HCL solation (A). Pasteurized milk (B) and local milk (C) was investigated by similar method, but in the five different concentration (0.01 µM, 0.001 µM, 0.0001 µM and 0.00000001 µM). All of the tests were carry out in the Ferrocyanide/ ferricyanide solution with scan rate 0.1 V/s, modulation amplitude 0.025 V, interval time 0.05 and in the range of -0.5 V to +1 V.

View Article Online
DOI: 10.1039/C9AY01185D

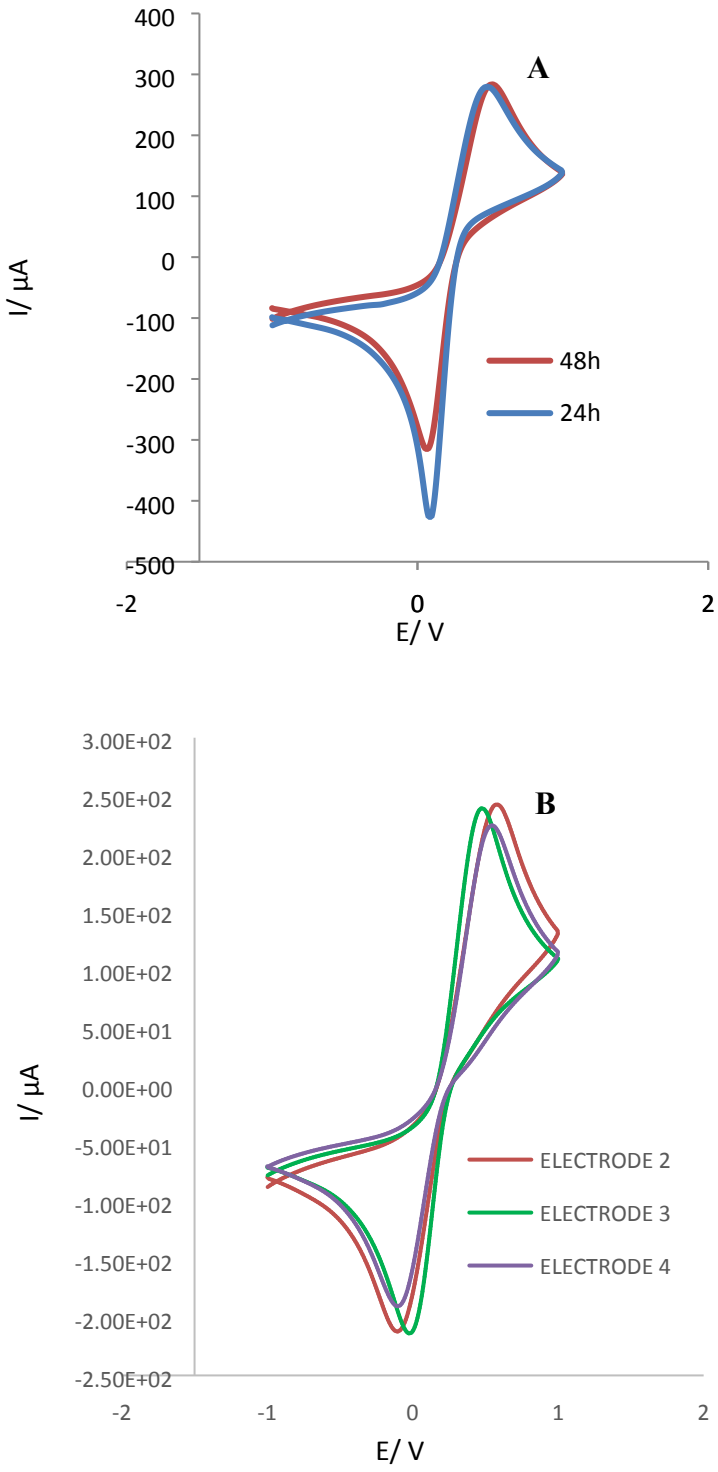

Fig. 5. **A)** CVs of GQDs-CS/KCC-1-NH_2-Tb/Aptamer in different storage time. **B)** CVs of thee electrode in similar conditions.

View Article Online
DOI: 10.1039/C9AY01185D

Table 1. Comparison of the analytical parameters of some electrochemical aptasensors for the detection of AFM1.

Type of biosensor	Strategy	LOD	Dynamic range	Ref
Electrochemical Sensors	Apt-modified SPGE with CS-modified AUNPs	0.9 ng/L	2-600 ng/L	[29]
	DNA-aptamer s immobilized on a carbon screen-printed electrode	1.15 ng/L	2-150 ng/L	[30]
	Label-free aptamer-AFM1 on Fe_3O_4/PANi	1.98 ng/L	6–60 ng/L	[31]
	GQDs-CS/KCC-1-NH_2-Tb-Aptamer labeled by toluidine blue	1 fM	0.1 µM-1 fM	This work

Table 2. Compartment the analytical parameters of different methods to determination of the AFM1.

Type of biosensor	Strategy	LOD	Dynamic range	Ref
ELISA	monoclonal antibody	0.04 ng/ml	0.16- 0.50 ng/ml	[32]
	Polyclonal antibodies	1.0 ng/ml	0.018-0.038 ng/ml	[33]
	Immunoscreen AFLA	4.3 ng/ml	4.3-91.8 ng/ml	[34]
	Immobilization of the specific antibodies on the screen-printed electrode	25 ng/ml	30–160 ng/ml	[35]
	An amperometric immunosensor based on the gold-labeled antibodies immobilized at screen-printed electrodes	15ng/ml	15–1000ng/ml	[36]
	A screen-printed electrode array adapted with a standard 96-well microplate	1ng/ml	5–250ng/ml	[37]
BERA	Membrane-engineering	5 pg/ml	5-500 pg/ml	[38]
HPLC	Sep-Pak1 silica cartridge	10 pg/ml	10-500 pg/ml	[39]
	solid phase extraction on OASIS HLB	0.006 mg/kg	0.050-0.250 mg/kg	[40]
EC	Milk sample	1 fM	0.1 µM-1 fM	This work

View Article Online
DOI: 10.1039/C9AY01185D